Strong Precursor-Pore Interactions Constrain Models for Mitochondrial Protein Import

Jean-François Chauwin,* George Oster,* and Benjamin S. Glick#
*Department of Molecular and Cellular Biology, University of California, Berkeley, California 94720-3112, and #Department of Molecular Genetics and Cell Biology, The University of Chicago, Chicago, Illinois 60637 USA

ABSTRACT Mitochondrial precursor proteins are imported from the cytosol into the matrix compartment through a proteinaceous translocation pore. Import is driven by mitochondrial Hsp70 (mHsp70), a matrix-localized ATPase. There are currently two postulated mechanisms for this function of mHsp70: 1) The "Brownian ratchet" model proposes that the precursor chain diffuses within the pore, and that binding of mHsp70 to the lumenal portion of the chain biases this diffusion. 2) The "power stroke" model proposes that mHsp70 undergoes a conformational change that actively pulls the precursor chain through the pore. Here we formulate these two models quantitatively, and compare their performance in light of recent experimental evidence that precursor chains interact strongly with the walls of the translocation pore. Under these conditions the simulated Brownian ratchet is inefficient, whereas the power stroke mechanism seems to be a plausible description of the import process.

INTRODUCTION

Most proteins of the mitochondrial matrix are synthesized as cytosolic precursors, which are imported through a proteinaceous pore that spans the two mitochondrial membranes (Lill et al., 1996). The signal that targets a precursor protein to the matrix resides within an N-terminal presequence (Schatz and Dobberstein, 1996). Precursors must be unfolded to pass through the translocation pore, and precursor polypeptides can assume an extended conformation within the pore (Rassow et al., 1990). Protein import across the inner membrane is driven by ATP inside the matrix (Hwang and Schatz, 1989; Wachter et al., 1994), where the corresponding ATPase is the matrix-localized mitochondrial Hsp70 protein (mHsp70) (Kang et al., 1990; Scherer et al., 1990).

Soon after the identification of mHsp70 as the translocation ATPase, it was postulated that protein import is driven by a "Brownian ratchet" mechanism (Neupert et al., 1990; Simon et al., 1992). According to this model, a precursor chain diffuses within the translocation pore; soluble mHsp70 molecules bind to the chain on the matrix side of the pore, thereby hindering reverse diffusion and causing a net unidirectional movement of the chain into the matrix. A quantitative study suggested that this mechanism could account for the observed rates of translocation (Simon et al., 1992; Peskin et al., 1993). However, three subsequent findings have forced a rethinking of the original ratchet model: 1) mHsp70 drives translocation in conjunction with Tim44, a membrane-associated subunit of the inner membrane import machinery (Rassow et al., 1994; Kronidou et al., 1994; Schneider et al., 1994). 2) Some precursors fold before import, and their unfolding can be accelerated by the ATP-dependent action of mHsp70 (Glick et al., 1993; Voos et al., 1993; Stuart et al., 1994). 3) The diffusion of precursor proteins within the translocation pore is far slower than originally assumed (see below). Attempts have been made to incorporate the first two findings into updated versions of the Brownian ratchet model (Stuart et al., 1994; Mayer et al., 1995), but the third finding has not previously been examined.

The recent data prompted us and others to suggest an alternative model for the action of mHsp70 during protein translocation. According to this view, mHsp70 undergoes a conformational change ("power stroke") while bound simultaneously to Tim44 and to the precursor chain (Glick, 1995; Pfanner and Meijer, 1995). This power stroke would exert an inward pulling force on the chain, thereby driving the unfolding and import of the precursor protein. In other words, mHsp70 would be functionally analogous to motor proteins such as myosin. Qualitative arguments have been advanced in favor of the power stroke model (Horst et al., 1997), but a quantitative analysis has been lacking. Here we formulate the power stroke model quantitatively in such a way that it can be compared with the Brownian ratchet model.

MODELS

The membrane potential ($\Delta\Psi$) across the mitochondrial inner membrane drives the initial penetration of presequences into the matrix (Schleyer and Neupert, 1985). Subsequent import of a precursor chain is independent of $\Delta\Psi$ but requires the ATPase function of mHsp70 (Hwang et al., 1991; Ungermann et al., 1996). In this work we address only the $\Delta\Psi$-independent, mHsp70-dependent phase of protein translocation.

Based on the conventions of polymer physics, a precursor polypeptide can be modeled as a chain of amino acid

Received for publication 6 August 1997 and in final form 8 January 1998.
Address reprint requests to Dr. Benjamin S. Glick, The University of Chicago, 920 East 58th St., Chicago, IL 60637. Tel.: 773-702-5315; Fax: 773-702-3172; E-mail: bsglick@midway.uchicago.edu.

0006-3495/98/04/1732/12 $2.00

"beads" connected by elastic springs, i.e., a Rouse chain (Doi and Edwards, 1986). Segments of the chain that are outside the pore can bend. Because this bending will not significantly affect translocation times, we chose to model a precursor chain in the pore as a semirigid rod (Fig. 1; Appendix A). This approach has the disadvantage of neglecting effects due to extension and compression of the precursor chain (see Discussion), but it has the advantage of greatly simplifying the computations.

Driven by Brownian forces, a precursor chain will diffuse through the translocation pore. In the simplest case, suppose that the chain diffuses freely and does not interact with the walls of the pore. The diffusion constant, D, for such a freely diffusing chain is $\sim 10^{-8}$ cm^2/s (see Appendix B) (Simon et al., 1992; Peskin et al., 1993). How long would it take the chain to diffuse the length of the pore under these conditions? The translocation pore spanning the two mitochondrial membranes is ~20 nm long (Rassow et al., 1990); thus the average time for the chain to diffuse $x = 20$ nm would be $\sim\langle x^2\rangle/2D \approx 0.2$ ms.

This value does not agree with the experimental data, which indicate that the time required for a precursor chain to diffuse the length of the translocation pore is on the order of minutes, not milliseconds. One relevant experiment involves an artificial precursor, pCoxIV-dihydrofolate reductase (pCoxIV-DHFR), consisting of a mitochondrial presequence fused to mouse dihydrofolate reductase (Hurt et al., 1984). When denatured pCoxIV-DHFR is incubated with mitochondria in which mHsp70 has been inactivated, the presequence inserts into the translocation pore but then becomes stuck. This precursor remains trapped in the pore for tens of minutes, neither falling back out of the mitochondrion nor diffusing far enough into the matrix for the presequence to be cleaved (Hwang et al., 1991; Glick et al., 1992). A similar phenomenon is observed with the related precursor pSu9(1-69)-DHFR (Wachter et al., 1992; Gambill et al., 1993). Recently, an elegant experimental system has been devised to examine the diffusion of DHFR fusion proteins in the translocation pore (Ungermann et al., 1994, 1996). Experiments performed with this system yielded mean times of ~5–15 min for a 20-nm segment of precursor chain to diffuse backward out of the pore. As described in Appendix B, these data can be used to calculate an "effective" diffusion constant, D_{eff}, for the chain. If a 20-nm chain segment requires an average of 5 min to diffuse backward out of the pore, then D_{eff} is computed to be $\sim 2 \times 10^{-15}$ cm^2/s.

How do we explain the finding that this measured value of D_{eff} is more than 10^6-fold lower than the calculated diffusion coefficient for a freely diffusing chain? Evidently the precursor chain in the translocation pore is not free to diffuse, but is hindered by interactions of the chain with the walls of the pore. Although this phenomenon is poorly understood, it presumably involves a combination of electrostatic, van der Waals, hydrogen bonding, and hydrophobic interactions (Creighton, 1993). To formulate translocation models that are biologically relevant, it is essential to take these drag forces into account.

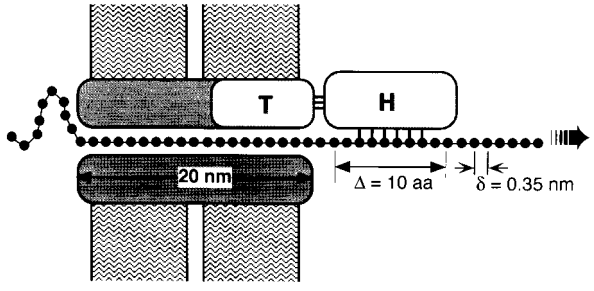

FIGURE 1 Schematic of the translocation model. The translocation pore spans the two mitochondrial membranes from the cytosol (*left*) to the matrix (*right*). We assume that the precursor chain segment in the pore is unfolded, and that the chain passes through the pore one amino acid at a time. T = *T*im44, H = m*H*sp70. $\Delta \approx 3.5$ nm is the length of the "footprint," the region occluded when mHsp70 binds to the precursor chain. $\delta = 0.35$ nm, the distance between α-carbons in an extended polypeptide chain.

The Brownian ratchet model

The original Brownian ratchet model assumed that an incoming precursor chain would be bound by soluble mHsp70 molecules (Neupert et al., 1990; Simon et al., 1992). However, it has become clear that mHsp70 acts in conjunction with the membrane partner protein Tim44 (Rassow et al., 1994; Kronidou et al., 1994; Schneider et al., 1994) and the nucleotide exchange factor mGrpE (Bolliger et al., 1994; Laloraya et al., 1994; Nakai et al., 1994). In addition, more information is now available about how nucleotides modulate the interactions of mHsp70 with polypeptides and with Tim44 and mGrpE (McCarty et al., 1995; von Ahnsen et al., 1995; Horst et al., 1996; Schneider et al., 1996; Miao et al., 1997; Azem et al., 1997; Dekker and Pfanner, 1997). We have incorporated these findings into a revised version of the Brownian ratchet model. The goal was to design a hypothetical ratchet mechanism that is as efficient as reasonably possible, given our current understanding of the system.

The kinetic cycle for the Brownian ratchet is shown in Fig. 2. The overall scheme for the mHsp70 reaction cycle is based on studies of DnaK and related chaperones (Szabo et al., 1994; Greene et al., 1995; McCarty et al., 1995; Pierpaoli et al., 1997); Appendix C contains additional details about the assumptions underlying the model. We begin our study when the precursor chain is already threaded through the translocation pore. The cycle starts in state 1, with mHsp70 in solution and complexed with ATP. The chain is free to diffuse bidirectionally in the channel. mHsp70 · ATP undergoes a reversible binding to both Tim44 and the chain to yield state 2, at which point the chain is immobilized. (Strictly speaking, the binding to Tim44 and the precursor chain must be sequential; however, we assume that both bindings are fast, and so they can be considered simulta-

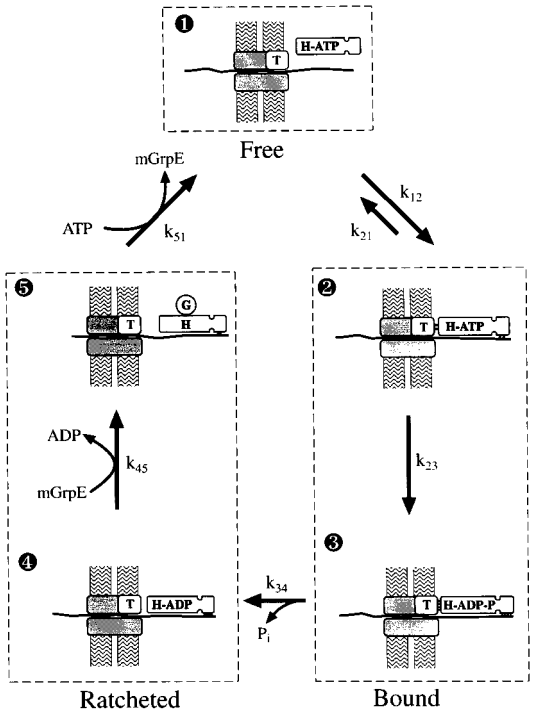

FIGURE 2 The Brownian ratchet kinetic cycle consists of five chemical states, which are grouped into three "dynamic" states labeled Free, Bound, and Ratcheted. The mean time in each state is given by the reciprocal of the rate constants leading out of the state. Thus the fraction of time the system spends in each dynamic state is given by $\tau_F = 1/k_{12}$, $\tau_B = 1/(k_{21} + k_{23}) + 1/k_{34}$, $\tau_R = 1/k_{45} + 1/k_{51}$. T, Tim44; H, mHsp70; G, mGrpE. Weak interactions between proteins are indicated by two bars, strong interactions by four bars.

neous.) mHsp70 then hydrolyzes ATP to generate state 3, in which mHsp70 · ADP · P_i is bound stably to both Tim44 and the chain. To allow diffusion of the chain, mHsp70 must now dissociate from Tim44 while remaining bound to the chain. We assume that P_i release triggers dissociation of mHsp70 · ADP from Tim44 (Schneider et al., 1996), yielding state 4. In state 4 the precursor chain is ratcheted: it can diffuse forward into the matrix, but the bound mHsp70 prevents it from diffusing backward.

The bound mHsp70 molecule will sterically hinder the attachment of a second mHsp70 molecule to Tim44 and to the precursor chain. However, after the chain has diffused a certain distance into the matrix, enough of the emerging chain will be exposed to the lumenal environment for a second mHsp70 molecule to bind. We define the minimal spacing between bound mHsp70 molecules as the "footprint length." This distance is not known precisely, but it must be at least as large as the mHsp70 peptide-binding cleft, which holds six or seven amino acids (Flynn et al., 1991; Blond-Elguindi et al., 1993; Zhu et al., 1996). We have chosen a footprint length of 3.5 nm, corresponding to ~10 amino acids of extended polypeptide chain.

Even when the chain has diffused by less than the footprint length, a second mHsp70 molecule can bind if the first mHsp70 molecule has already dissociated from the chain. Dissociation of mHsp70 from the chain is modeled as a two-step process (Fig. 2). First, mGrpE binds to mHsp70 and displaces ADP, thereby generating state 5. At this point mHsp70 is still bound to the chain, although this association may be weaker than in state 4 (Harrison et al., 1997). Subsequent binding of ATP displaces mGrpE from mHsp70 and leads to release of mHsp70 · ATP from the chain, returning the cycle to state 1.

In the Brownian ratchet model, the roles of the three key proteins can be summarized as follows: 1) mHsp70 serves to "capture" the precursor chain and bias its diffusion. 2) mGrpE acts as a nucleotide exchange factor to accelerate recycling of mHsp70 (Laloraya et al., 1995; Schneider et al., 1996; Miao et al., 1997; Dekker and Pfanner, 1997). 3) Tim44 has a dual function: (i) Like proteins of the DnaJ family, Tim44 probably accelerates ATP hydrolysis by mHsp70, thereby triggering stable binding of mHsp70 to the precursor chain (Liberek et al., 1991; McCarty et al., 1995; Rassow et al., 1994). Catalysis of the ATPase activity of mHsp70 may actually require both Tim44 and a precursor polypeptide (Karzai and McMacken, 1996); such an arrangement would ensure that ATP hydrolysis results in the productive interaction of mHsp70 with an incoming precursor. (ii) Tim44 targets mHsp70 to the segment of the chain that has just emerged from the translocation pore. The binding of mHsp70 at this position results in optimal ratcheting of the chain.

The power stroke model

The power stroke model is similar to the Brownian ratchet model in many respects (Fig. 3, Table 1). The major difference is that mHsp70 undergoes a conformational change while remaining bound to Tim44. Once again we have attempted to design a mechanism that is efficient, but also plausible and consistent with the experimental data (see Appendix C).

In state 1 of the power stroke model, mHsp70 is complexed with ATP and bound weakly to Tim44. In this state mHsp70 exists in a high-energy conformation, indicated by the cocked spring in Fig. 3. The immobilized mHsp70 · ATP undergoes a reversible binding to the chain to yield state 2. ATP hydrolysis then generates state 3, in which mHsp70 · ADP · P_i is bound stably to both Tim44 and the chain. The system now enters the power stroke phase of the cycle (Pierpaoli et al., 1997). By analogy to myosin (Spudich, 1994), we assume that the power stroke is triggered by P_i release, which allows mHsp70 to "relax" to a lower-energy conformation. This conformational change occurs in state 4. During the power stroke mGrpE can bind to mHsp70, displacing ADP to yield state 5. The power stroke terminates when ATP binds to mHsp70 and displaces mGrpE, causing release of mHsp70 · ATP from the chain and restoring the high-energy conformation of state 1.

In the power stroke model, the roles of the three key proteins can be summarized as follows: 1) mHsp70 pulls on

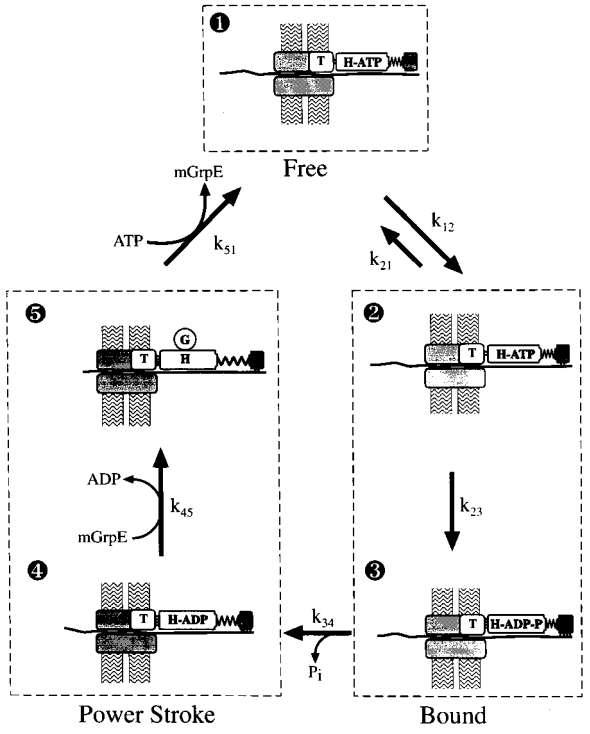

FIGURE 3 The power stroke kinetic cycle consists of five chemical states, which are grouped into three "dynamic" states labeled Free, Bound, and Power Stroke. For further details and symbol definitions, see Fig. 2.

the precursor chain, thereby driving import. 2) mGrpE acts as a nucleotide exchange factor to accelerate release of mHsp70 from the precursor chain. 3) Tim44 has a treble function: (i) As in the ratchet model, Tim44 catalyzes ATP hydrolysis by mHsp70. (ii) Tim44 allows force generation by serving as a membrane anchor for mHsp70 (Glick, 1995; Pfanner and Meijer, 1995). (iii) Immobilization of mHsp70 on Tim44 increases the relative concentrations of mHsp70 and the precursor chain, yielding stable binding of mHsp70, even to precursor peptide sequences that are not optimally recognized by this chaperone[1] (Flynn et al., 1991; Blond-Elguindi et al., 1993; Gragerov and Gottesman, 1994).

Translocation mechanics

Translocation times in the ratchet and power stroke models are computed by formulating dynamical equations for the motion of the precursor chain. The chain is subject to different forces in each of the kinetic states diagrammed in Figs. 2 and 3. Therefore, we have coupled the kinetic schemes for the mHsp70 reaction cycle to a mechanical model for diffusion of the chain within the translocation pore.

The velocity, v, of a chain diffusing through the pore can be described by the following stochastic force balance equation on the chain:

$$\underbrace{\zeta v}_{\text{Drag force}} = \underbrace{F_p}_{\text{Pore potential forces}} + \underbrace{F_R}_{\text{Ratchet force}} + \underbrace{F_{PS}}_{\text{Power stroke force}} + \underbrace{F_B}_{\text{Brownian force}} \quad (1)$$

Here the first term represents the drag force on the chain due to its viscous interactions with the pore. ζ, the drag on chain, is related to the diffusion coefficient by the Einstein relation: $D = k_B T/\zeta$, where k_B is Boltzmann's constant and T is the absolute temperature. F_p represents any velocity-independent forces the pore exerts on the chain in addition to the viscous drag force. (We have not included such velocity-independent forces in the simulations shown here, because the method described in Appendix B incorporates all pore forces into an effective diffusion coefficient, D_{eff}.) F_R is the "ratchet" force exerted when steric hindrance prevents the chain-mHsp70 complex from diffusing backward into the pore. In our calculations we have implemented this force as a "reflecting" boundary condition on the chain, as explained in Appendix D. F_{PS} is the force of the power stroke, which we model as the relaxation of a linear spring (Huxley and Simmons, 1971; Peskin and Oster, 1995). Thus the force exerted by mHsp70 is given by

$$F_{PS} = -k(x - x_0) \quad (2)$$

where k is the spring constant, x_0 is the total distance that would be covered by the power stroke if the spring were allowed to relax completely, and x is the distance that has actually been covered as the power stroke is under way. Finally, F_B is the "Brownian force" due to thermal fluctuations of the chain (see Appendix D).

In each kinetic state of the mHsp70 reaction cycle, we solve the equation of motion (Eq. 1) corresponding to the forces acting on the chain in that state. This calculation yields the displacement of the chain (i.e., the net translocation) in each state. From the viewpoint of the chain's motion, the kinetic states can be collected into three "dynamic" states, shown by the dashed boxes in Figs. 2 and 3 (see Appendix D). For the ratchet model these dynamic

TABLE 1 Range of rate constants for the Brownian ratchet and power stroke models

Rate constants (s^{-1})	
k_{12}	2–20
k_{21}	0.5–5
k_{23}	1–10
k_{34}	10–100
k_{45}	1–10*
k_{51}	0.2–2

See Figs. 2 and 3.
*In the power stroke model, k_{45} is multiplied by a factor that depends upon how far the power stroke has progressed (see Appendix C).

[1]Thanks to Andreas Matouschek for this insight.

states are called free, bound, and ratcheted (Fig. 4). The computational procedure for the power stroke model is similar, except that the dynamic states are free, bound, and power stroke.

COMPUTATIONS

Because detailed biochemical information is not yet available for the mHsp70 chaperone system, we tested a range of values for the parameters used in the simulations. The first test was to vary the kinetic rate constants for the steps in the mHsp70 reaction cycle. Our estimates for each of the rate constants spanned a 10-fold range (Table 1, Appendix C); for simplicity we varied all of these rate constants in parallel, thereby varying the total mHsp70 ATPase cycle time by a factor of 10. The symbol f denotes the fraction of the maximum possible cycle time, which we take as 5 s (see Appendix C). A mean time of ~2 s for the mHsp70 reaction cycle corresponds to $f = 0.4$, and our analysis focuses primarily on results obtained using $f = 0.4$. When computing translocation times as a function of f, we fixed the remaining parameters at values that seemed plausible (see below).

Fig. 5 shows three plots of computed translocation times as a function of f for the Brownian ratchet (BR) and power stroke (PS) models, where T denotes the average time required for a precursor chain to be translocated by 20 nm. In Fig. 5 *b* the effective diffusion coefficient D_{eff} was set at 2×10^{-15} cm^2/s. With this value of D_{eff}, a 20-nm chain segment would diffuse backward out of the pore in ~5 min, a number that is in the range of experimental measurements (see Models and Appendix B). For comparison, D_{eff} was also set at 2×10^{-14} cm^2/s (Fig. 5 *a*) and 3.7×10^{-16} cm^2/s (Fig. 5 *c*), corresponding to back-diffusion times for a 20-nm chain segment of 0.5 and 30 min, respectively.

Under most of the simulation conditions tested, the power stroke mechanism yields faster translocation than the Brownian ratchet. The extra force generated by the power stroke helps to overcome the drag forces in the pore. However, at high D_{eff} values—when the drag forces are weak, and diffusion is rapid—the ratchet can actually give faster translocation than the power stroke. The reason is that the ratchet mechanism allows an mHsp70 molecule to bind even before the previous mHsp70 molecule has dissociated, whereas the power stroke mechanism requires that mHsp70 complete its entire reaction cycle before beginning a new round of translocation.

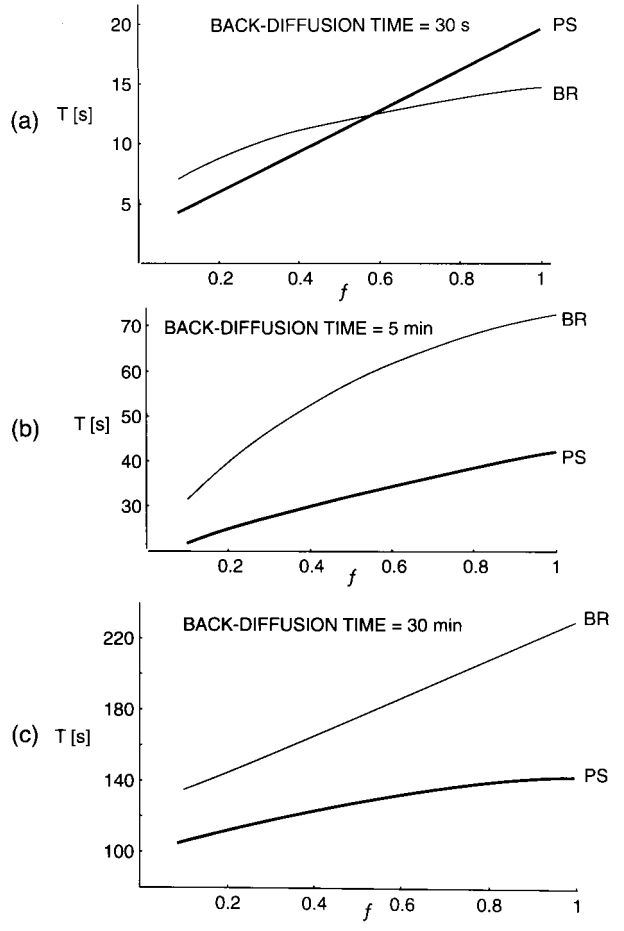

FIGURE 5 Translocation times (T) for a 20-nm chain segment in the Brownian ratchet (BR) and power stroke (PS) models as a function of the fraction (f) of the maximum mHsp70 ATPase cycle time. The effective diffusion coefficient D_{eff} was set at (*a*) 2×10^{-14} cm^2/s, (*b*) 2×10^{-15} cm^2/s, or (*c*) 3.7×10^{-16} cm^2/s.

To perform these calculations we had to choose appropriate values for several parameters other than the kinetic rate constants (Table 2). Our approach was to ensure that both of the translocation mechanisms are efficient, but rea-

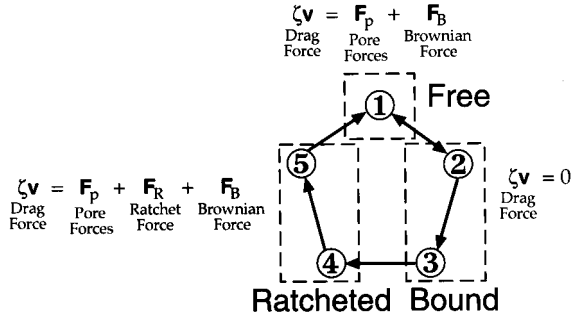

FIGURE 4 The computational scheme for the Brownian ratchet model. The mHsp70 reaction cycle is represented as a Markov chain linking five kinetic states, which are grouped into three dynamic states: Free (state 1), Bound (states 2 and 3), and Ratcheted (states 4 and 5). In each dynamic state, Eq. 1 is solved for an amount of time equal to the mean residence time in that state.

TABLE 2 Geometrical parameter values

Parameter	Value
δ = distance between amino acids	0.35 nm
L = length of translocation pore	20 nm
Δ = footprint length	3.5 nm
x_0 = length of power stroke	7.0 nm
k = spring constant for the power stroke	1.5 pN/nm

sonable (see Models). One important parameter for the Brownian ratchet model is the footprint length, Δ (see Fig. 1). As this distance decreases, ratcheting becomes more efficient and translocation is faster; indeed, for a "perfect ratchet" the translocation velocity is given simply as $v = 2D_{\text{eff}}/\Delta$ (Peskin et al., 1993). The minimum possible footprint length is ~2.5 nm, which is the size of the chain segment covered by the peptide-binding cleft of mHsp70 (Zhu et al., 1996). We chose a footprint length of 3.5 nm. In our model system the choice of Δ has little effect on the translocation rate (Fig. 6), because mHsp70 usually completes its reaction cycle before the chain has diffused a distance equivalent to the footprint length. For the power stroke model, a key parameter is the energy conversion efficiency, which represents the fraction of the ATP hydrolysis energy that is used productively to do work. If the power stroke goes to completion, the total work performed will be given by $\frac{1}{2}kx_0^2$, where k is the elastic constant of the spring and x_0 is the length of the power stroke. We set $k = 1.5$ pN/nm and $x_0 = 7$ nm, values that are in the range of those determined for myosin and kinesin (Coppin et al., 1995; Finer et al., 1994, 1995; Svodoba and Block, 1994). Under these conditions the energy conversion efficiency of the mHsp70 motor is ~45% (assuming a total ATP hydrolysis energy of $20k_BT = 12$ kcal/mol), also in the same range as the corresponding values for myosin and kinesin (Hunt et al., 1994). Altering the power stroke length would significantly change the efficiency of the mHsp70 motor (Fig. 6).

How do the computed translocation times shown in Fig. 5 compare with the experimental data? Empirically, complete import of a denatured 25-kDa mitochondrial precursor takes ≤60 s (Eilers et al., 1988; Matouschek et al., 1995). Such a precursor chain is ~80 nm long, implying that translocation of a 20-nm segment of chain requires ≤15 s. However, for $D_{\text{eff}} = 2 \times 10^{-15}$ cm^2/s and $f = 0.4$, the simulated Brownian ratchet yields a value of $T = 52$ s (Fig. 5 *b*). The simulated power stroke fares considerably better, giving $T = 29$ s under the same conditions (Fig. 5 *b*). As described in the Discussion, refinements of the model will almost certainly allow the simulated power stroke mechanism to match the experimentally observed translocation rates.

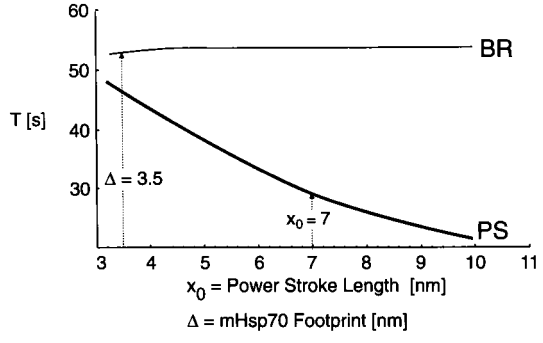

FIGURE 6 Translocation times (T) for a 20-nm chain segment in the Brownian ratchet (BR) and power stroke (PS) models as a function of the footprint length (Δ) or the power stroke length (x_0), respectively. For these simulations we used $D_{\text{eff}} = 2 \times 10^{-15}$ cm^2/s and $f = 0.4$. Arrows indicate the values of $\Delta = 3.5$ nm and $x_0 = 7$ nm that were used in the standard simulations.

DISCUSSION

A theoretical approach will not by itself reveal how proteins are imported into mitochondria. However, this kind of analysis serves two purposes. First, it helps to define possible translocation mechanisms that are consistent both with the experimental data and with the laws of mechanics. Second, it highlights questions that will generate further insights into the import process.

The major conclusion of this study is that the interactions of precursor proteins with the translocation pore are very significant. Based on existing experimental systems, we developed a simple mathematical procedure to calculate diffusion coefficients for precursor chains in the translocation pore. Remarkably, the calculated diffusion coefficients are ~10^6-fold lower than for a freely diffusing chain. This phenomenon has received little attention, but it must be incorporated into any mechanistic description of translocation. Strong drag forces in the pore greatly reduce the predicted efficiency of a Brownian ratchet, and under these conditions a power stroke motor could outperform a Brownian ratchet.

Even our simulated power stroke motor does not match the translocation rates observed in actual mitochondria, indicating that the current translocation model is too simplistic. We must therefore examine two key assumptions underlying this model. The first assumption is that precursor-pore interactions exert a drag force of constant magnitude. In reality, different segments of the precursor chain will interact differently with the pore walls. We performed simulations in which the precursor chain experienced occasional strong resistance instead of a constant, moderate drag force. This modification had virtually no effect on translocation rates in the ratchet model, but it significantly accelerated translocation in the power stroke model (not shown). Additional experiments are needed to characterize how the strength of the drag force varies as different segments of the chain enter the pore.

The second important assumption is that the chain segment in the pore is fully extended, capable neither of compression nor of further extension. In fact, the mitochondrial translocation pore is quite flexible (Vestweber and Schatz, 1988b, 1989), and translocating precursor chains may be able to form α-helices or other elements of secondary structure. Hence it would be more accurate to model the precursor as a Rouse chain (a series of beads connected by elastic springs) than as a rigid rod. This modification would probably make little difference in the Brownian ratchet model, but in the power stroke model it would be expected to accelerate translocation, for the following reason. With the rigid rod assumption, if a precursor chain experiences multiple interactions with the pore walls, the power stroke must

break all of these interactions simultaneously. But if the chain were extensible, the power stroke could act sequentially to break different sets of interactions. Future simulations will examine the Rouse chain concept in more detail.

Are there modifications to the Brownian ratchet model that would make this mechanism more effective? The strength of the simulated Brownian ratchet is inversely proportional to the size of the ratcheting interval, which is the distance the chain diffuses between the binding of successive mHsp70 molecules (Peskin et al., 1993). With a very small ratcheting interval it would be possible to overcome the drag forces caused by strong pore interactions. For comparison, Wang et al. (1997) have recently shown that the extraordinarily high stall force of RNA polymerase (~30 pN) can be accounted for by a ratchet mechanism with a ratcheting interval the size of a single nucleotide (0.34 nm). However, based on the known properties of the mitochondrial translocation machinery, it seems unlikely that such a small ratcheting interval could be achieved in this system.

Is our power stroke model a plausible representation of mHsp70 function? Because the drag forces in the pore are so powerful, we have assumed that mHsp70 is an efficient motor, comparable to myosin or kinesin. Although this assumption is not unreasonable, it is untested—for example, no information is yet available about the putative mHsp70 power stroke. But even if this power stroke turns out to be weaker than we have assumed, it is conceivable that two mHsp70 molecules can pull simultaneously on the precursor chain (Bömer et al., 1997). The strength of the mHsp70 motor could be examined directly by adapting optical laser trap technology (Vale, 1994) to study protein translocation into mitochondria or submitochondrial particles. A separate issue concerns the ATPase cycle time of mHsp70. The power stroke motor must turn over between strokes; therefore, to be compatible with the observed translocation rates, the ATPase cycle time for the complete mHsp70 chaperone system (including Tim44, mGrpE, and a precursor chain) must be <5 s. This number can be measured once all of the components of the mHsp70 chaperone system become available in purified form.

Although our computations favor a power stroke mechanism, they do not allow us to distinguish conclusively between the Brownian ratchet and power stroke models. Such a distinction will come from other lines of investigation. For example, most studies have focused on measurements of average translocation times, but additional mechanistic information could be obtained by examining the variances of translocation times (Svodoba et al., 1994; Schnitzer and Block, 1995; Wang et al., 1997). A second approach focuses on the details of the mHsp70 reaction cycle (Horst et al., 1996, 1997). In the Brownian ratchet model, mHsp70 must dissociate from Tim44 while remaining bound to the precursor chain (Fig. 2); whereas in the power stroke model, mHsp70 must remain bound to both Tim44 and the precursor chain (Fig. 3). These possibilities are being tested, but a consensus has yet to be reached (von Ahnsen et al., 1995; Horst et al., 1996; Schneider et al., 1996).

One of the most promising ways to examine the mechanism of translocation is to characterize the mHsp70-dependent unfolding of precursor proteins. Indeed, the power stroke notion was inspired by the finding that mHsp70 could unfold a stably folded precursor protein (Glick et al., 1993; Voos et al., 1993; Glick, 1995; Pfanner and Meijer, 1995). Although the models presented here assume that the precursor chain is already unfolded, they could be extended to incorporate an unfolding event. It seems likely that mHsp70 causes unfolding by pulling on the N-terminus of a folded domain (Matouschek et al., 1997). This novel reaction could be fruitfully examined by a combined theoretical and experimental study.

We have tried to delineate the most important mechanical factors that govern the translocation of proteins across the mitochondrial membranes. Elucidating the mechanism of this reaction will require supplementing biochemical and cell biological approaches with biophysical analyses. We hope that the present work provides a step in this direction.

APPENDIX A: ENTROPIC COILING OF THE CHAIN CAN BE NEGLECTED

When a flexible precursor chain enters the translocation pore, it must be straightened, and when the chain exits the pore it may become free to bend and coil once again. These processes involve entropic changes that could potentially alter the diffusion rate of the chain. Park and Sung (1996) computed the effect of entropic coiling on the diffusion of a freely translocating chain through a membrane pore. By considering the statistics of a Rouse (freely jointed) chain of N subunits, each of length b, constrained to pass through a membrane pore, they computed the force on the chain as a function of the number of sites, n, that have translocated through the pore:

$$F_{\text{chain}} = -\frac{dG}{dn} = \frac{k_B T}{2b}\left(\frac{1}{N-n} - \frac{1}{n}\right) \qquad \text{(A1)}$$

In our simulations of translocation the pore length is 20 nm, which corresponds to ~60 amino acids, and the pore is always entirely occupied by a segment of precursor chain. Thus, in Eq. A.1, $60 \le n \le N - 60$, so $|F_{\text{chain}}| \le k_B T/2b(1/60)$. By estimating $b = 0.35$ nm (the length of a single amino acid unit in an extended polypeptide chain), it can be inferred that $|F_{\text{chain}}| \le 0.1$ pN. Because the other forces involved in translocation are much stronger than 0.1 pN, entropic coiling forces can be neglected.

In actuality, portions of the precursor chain that are outside the pore may not be random coils, but may be either folded into secondary structures or bound to other proteins (such as chaperones or import receptors). In this case the entropic coiling forces would be even smaller than those estimated above. Such interactions of external portions of the precursor would contribute to the drag forces opposing the diffusion of the chain through the pore.

In our calculations we have treated the chain as a semirigid rod; that is, its persistence length, λ, is longer than the pore length. λ is related to the bending modulus, B, of the chain by $\lambda = Bk_B T$, where k_B is Boltzmann's constant and T is the absolute temperature (Doi and Edwards, 1986).

APPENDIX B: ESTIMATION OF DIFFUSION COEFFICIENTS

To estimate diffusion coefficients for precursor chains in the mitochondrial translocation pore, we used data obtained from the experimental system

developed by Ungermann and co-workers (Ungermann et al., 1994, 1996). This system measures "backsliding" of DHFR fusion proteins in the pore in the absence of mHsp70 function. The DHFR domain is linked to a presequence that can insert into the pore, but translocation of the DHFR domain is blocked because the folded structure has been stabilized with methotrexate. In the simplest case, the segment of the presequence that reaches the matrix is cleaved off by the matrix processing peptidase, preventing further binding of mHsp70. Alternatively, mHsp70 can be inactivated by depleting the matrix of ATP. The result is that the precursor eventually falls back out of the mitochondrion: the folded DHFR domain blocks forward diffusion of the chain, but reverse diffusion can still take place. Fig. 7 shows the experimental setup.

The experiment can be represented mathematically as follows. We start with a population of chains located at $x = 0$ and write a diffusion equation for $P(x, t)$, the probability of a chain being at position x at time t on the domain $0 \le x \le L$, where L is the length of the chain. As a first approximation, we neglect the end effect that reduces the diffusion coefficient when the chain is only partially inserted into the pore, so we treat the diffusion coefficient, D, as a constant:

$$\frac{\partial P}{\partial t} = D\,\frac{\partial^2 P}{\partial x^2} \tag{B1}$$

The boundary conditions are: 1) The chain cannot penetrate the pore deeper than the point at which folded DHFR reaches the entrance of the translocation channel. This condition makes $x = 0$ a reflecting boundary. 2) We assume that once a chain has diffused out of the pore, it cannot reenter again. This condition makes the boundary at $x = L$ absorbing. Thus the boundary conditions on Eq. B.1 are

$$\begin{aligned} &\frac{\partial P}{\partial x}(x = 0, t) = 0, \quad \text{Reflecting} \\ &P(x = L, t) = 0, \quad \text{Absorbing} \end{aligned} \tag{B2}$$

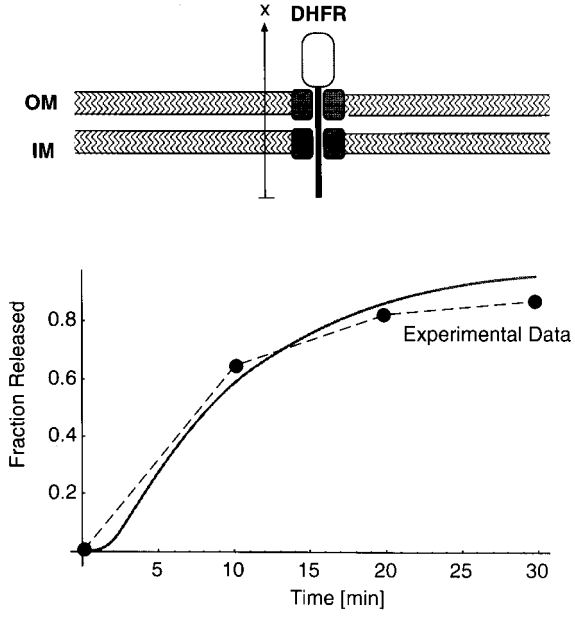

FIGURE 7 Estimating D_{eff}. (*Top*) Experimental setup. OM, outer mitochondrial membrane; IM, inner mitochondrial membrane. (*Bottom*) Least-squares fit of the diffusion model to data from figure 2B of Ungermann et al. (1996) for the pSu9(1-86)-DHFR precursor in the absence of matrix ATP. End effects were included in the calculation. The solid line shows a theoretical plot, using $D_{\text{eff}} = 10^{-15}$ cm^2/s.

The initial conditions are that all of the chains start in their fully inserted configuration:

$$P(x, t = 0) = \delta(x), \tag{B3}$$

where $\delta(x)$ is the Dirac delta function.

Equations B.1–B.3 can be solved via separation of variables and the solution expressed as a Fourier series:

$$P(x, t) = \sum_{n=0}^{\infty} \frac{2}{L}\, e^{-\lambda_n t} \cos\left(\frac{(2n+1)\pi}{2L}\, x\right), \tag{B4}$$

where the eigenvalues, λ_n, are

$$\lambda_n = \frac{\pi^2 D}{4L^2}(2n+1)^2. \tag{B5}$$

The probability of remaining in the interval $(0, L)$ at time t is $\int_0^L P(x', t)\mathrm{d}x'$, and so the probability of escaping from the pore by time t is

$$\text{Prob(Escape at } t) = 1 - \int_0^L P(x', t)\mathrm{d}x'. \tag{B6}$$

This function contains the diffusion coefficient as a parameter. For the data plotted in Fig. 7, a least-squares fit gives an estimated $D \approx 3 \times 10^{-15}$ cm^2/s for $L = 20$ nm.

End effects

As the chain backs out of the pore, the segment of precursor chain interacting with the pore will become progressively smaller, and therefore the diffusion coefficient will increase. To include this effect, Eq. B.2 is replaced by

$$\frac{\partial P}{\partial x} = \frac{\partial}{\partial x}\left(D(x)\frac{\partial P}{\partial x}\right). \tag{B7}$$

The diffusion coefficient is related to the drag coefficient, ζ, by $D = k_B T/\zeta$. Then for a chain of length L that has backed out of the pore a distance x, the drag coefficient is $\zeta(x) = \zeta_{\text{free}}(x/L) + \zeta_{\text{pore}}(1 - x/L)$, where ζ_{free} is the drag coefficient for the free chain and ζ_{pore} is the drag coefficient for the chain inside the pore. Therefore, the composite diffusion coefficient is

$$D(x) = \frac{k_B T}{\zeta_{\text{free}}\left(\dfrac{x}{L}\right) + \zeta_{\text{pore}}\left(\dfrac{L - x}{L}\right)}. \tag{B8}$$

It is easy to show that including the end effect results in a diffusion coefficient:

$$D = \frac{1}{\dfrac{2}{3}\left(\dfrac{1}{D_{\text{free}}}\right) + \dfrac{1}{3}\left(\dfrac{1}{D_{\text{pore}}}\right)}. \tag{B9}$$

Note that $D_{\text{free}} \gg D_{\text{pore}}$ (see below), so that $D_{\text{pore}} \approx D/3$. Thus, D_{pore} for the data of Fig. 7 is $\sim 10^{-15}$ cm^2/s. In our calculations we have used $D_{\text{eff}} \approx D_{\text{pore}}$, as computed above. (In general, if the diffusion coefficient of the free chain is known, then the above procedure can be used to estimate $D_{\text{pore}} = k_B T/\zeta_{\text{pore}}$, where $\zeta_{\text{pore}} = 3\,(k_B T)/D - 2\zeta_{\text{free}}$.)

Free diffusion of a chain in the pore

If a precursor chain were to diffuse unhindered through the translocation pore, the diffusion coefficient can be estimated as follows. Let L be the length of the pore (20 nm), d_P be the diameter of the pore (0.6 nm), d_C be the diameter of the cylindrical chain (0.5 nm), h be the size of the gap between the chain and the pore wall (0.05 nm), μ be the viscosity of the fluid (0.01 poise), and v be the velocity of the cylindrical chain through the pore. The velocity gradient across the gap is v/h, so the drag force per unit area is $(\mu v/h)$. Because the surface area of the cylindrical chain is $\pi d_C L$, the total drag force is

$$f = \mu(v/h)\pi d_C L$$

Thus the friction coefficient is

$$\zeta = f/v = \mu\pi d_C L/h \approx \mu\pi d_P L/h$$

For an extended polypeptide chain, $d_C \approx 0.5$ nm. It has been observed that the mitochondrial inner membrane remains impermeable to ions during translocation (Vestweber and Schatz, 1988a; Wienhues et al., 1991), implying that the pore is not substantially wider than the translocating precursor chain; thus we can estimate $d_P \approx 0.6$ nm. Then,

$$\begin{aligned} D_{\text{free}} &= k_B T/\zeta \\ &= (4\ \text{pN-nm})/[(0.01\ \pi\ \text{poise}) \times (0.5\ \text{nm}) \\ &\qquad \times (20\ \text{nm})/(0.05\ \text{nm})] \\ &= 6.5 \times 10^{-8}\ \text{cm}^2/\text{s}. \end{aligned}$$

Thus we see that the diffusion coefficient estimated from the data is much smaller than that estimated for a freely diffusing chain.

APPENDIX C: KINETIC SCHEMES AND RATE CONSTANTS

Kinetic schemes

As previously described (Schneider et al., 1996; Horst et al., 1997), the hypothetical reaction cycles shown in Figs. 2 and 3 are based on studies of mHsp70 and its partner proteins, and on studies of related Hsp70 chaperones. For the Brownian ratchet model, we incorporated the suggestion that release of inorganic phosphate facilitates the dissociation of mHsp70 from Tim44 (Schneider et al., 1996). For the power stroke model, we modified our earlier scheme (Horst et al., 1997) by assuming that mHsp70 never dissociates from Tim44—the power stroke mechanism does not require dissociation of the mHsp70-Tim44 complex, and in any case this dissociation reaction seems to be relatively slow (Horst et al., 1996).

To formulate equations describing the kinetic schemes, we shall use the following abbreviations: H is mHsp70, the matrix-localized mitochondrial Hsp70 chaperone; T is Tim44, the translocation pore component to which mHsp70 binds; C is the precursor polypeptide chain; G is mGrpE, the nucleotide exchange factor for mHsp70; ATP, ADP, P are nucleotides and inorganic phosphate. The kinetic cycle for the Brownian ratchet model can be summarized as follows:

$$\mathrm{T} + \underbrace{\mathrm{H}\cdot\mathrm{ATP}}_{\text{State 1}} + \mathrm{C} \underset{k_{21}}{\overset{k_{12}}{\rightleftharpoons}} \underbrace{\mathrm{T}-\mathrm{H}\cdot\mathrm{ATP}-\mathrm{C}}_{\text{State 2}} \tag{C1}$$

$$\underbrace{\mathrm{T}-\mathrm{H}\cdot\mathrm{ATP}-\mathrm{C}}_{\text{State 2}} \overset{k_{23}}{\longrightarrow} \underbrace{\mathrm{T}-\mathrm{H}\cdot\mathrm{ADP}\cdot\mathrm{P}-\mathrm{C}}_{\text{State 3}} \tag{C2}$$

$$\underbrace{\mathrm{T}-\mathrm{H}\cdot\mathrm{ADP}\cdot\mathrm{P}-\mathrm{C}}_{\text{State 3}} \overset{k_{34}}{\longrightarrow} \mathrm{T} + \underbrace{\mathrm{H}\cdot\mathrm{ADP}-\mathrm{C}}_{\text{State 4}} + \mathrm{P} \tag{C3}$$

$$\underbrace{\mathrm{H}\cdot\mathrm{ADP}-\mathrm{C}}_{\text{State 4}} + \mathrm{G} \overset{k_{45}}{\longrightarrow} \underbrace{\mathrm{H}-\mathrm{C}-\mathrm{G}}_{\text{State 5}} + \mathrm{ADP} \tag{C4}$$

$$\underbrace{\mathrm{H}-\mathrm{C}-\mathrm{G}}_{\text{State 5}} + \mathrm{ATP} \overset{k_{51}}{\longrightarrow} \underbrace{\mathrm{H}\cdot\mathrm{ATP}}_{\text{State 1}} + \mathrm{C} + \mathrm{G} \tag{C5}$$

The kinetic cycle for the power stroke model can be summarized as follows, where H* represents the high-energy conformation of mHsp70:

$$\underbrace{\mathrm{T}-\mathrm{H}^*\cdot\mathrm{ATP}}_{\text{State 1}} + \mathrm{C} \underset{k_{21}}{\overset{k_{12}}{\rightleftharpoons}} \underbrace{\mathrm{T}-\mathrm{H}^*\cdot\mathrm{ATP}-\mathrm{C}}_{\text{State 2}} \tag{C6}$$

$$\underbrace{\mathrm{T}-\mathrm{H}^*\cdot\mathrm{ATP}-\mathrm{C}}_{\text{State 2}} \overset{k_{23}}{\longrightarrow} \underbrace{\mathrm{T}-\mathrm{H}^*\cdot\mathrm{ADP}\cdot\mathrm{P}-\mathrm{C}}_{\text{State 3}} \tag{C7}$$

$$\underbrace{\mathrm{T}-\mathrm{H}^*\cdot\mathrm{ADP}\cdot\mathrm{P}-\mathrm{C}}_{\text{State 3}} \overset{k_{34}}{\longrightarrow} \underbrace{\mathrm{T}-\mathrm{H}\cdot\mathrm{ADP}-\mathrm{C}}_{\text{State 4}} + \mathrm{P} \tag{C8}$$

$$\underbrace{\mathrm{T}-\mathrm{H}\cdot\mathrm{ADP}-\mathrm{C}}_{\text{State 4}} + \mathrm{G} \overset{k_{45}}{\longrightarrow} \underbrace{\mathrm{T}-\mathrm{H}-\mathrm{C}-\mathrm{G}}_{\text{State 5}} + \mathrm{ADP} \tag{C9}$$

$$\underbrace{\mathrm{T}-\mathrm{H}-\mathrm{C}-\mathrm{G}}_{\text{State 5}} + \mathrm{ATP} \overset{k_{51}}{\longrightarrow} \underbrace{\mathrm{T}-\mathrm{H}^*\cdot\mathrm{ATP}}_{\text{State 1}} + \mathrm{C} + \mathrm{G} \tag{C10}$$

Rate constants

To estimate the rate constants for the mHsp70 ATPase reaction cycle (Table 1), we relied primarily on kinetic studies of the DnaK chaperone system, which is closely related to the mHsp70 system (Boorstein et al., 1994; Rensing and Maier, 1994; Bolliger et al., 1994; Nakai et al., 1994; Laloraya et al., 1994; Rowley et al., 1994):

- The total ATPase cycle time was estimated to be ~2 s. This time is slightly shorter than for the DnaK chaperone system, in which the minimal ATPase cycle time is ~3–6 s (Jordan and McMacken, 1995; McCarty et al., 1995).
- The rate constant k_{12} for binding of mHsp70 to the precursor chain was estimated to be 2–20 s^{-1} by assuming that the concentration of mHsp70 in the matrix is ~5–50 μM (Kronidou et al., 1994; Schneider et al., 1994; Rassow et al., 1994) and that the second-order binding rate constant for an mHsp70-peptide interaction is $\sim 4 \times 10^5$ M^{-1} s^{-1} (Schmid et al., 1994).
- The rate constant k_{21} for the dissociation of mHsp70 · ATP from the precursor chain was estimated to be 0.5–5 s^{-1}, based on measured rate constants for DnaK-peptide dissociation (Schmid et al., 1994; Pierpaoli et al., 1997).
- The rate constant k_{23} for γ-phosphate cleavage by mHsp70 was estimated to be 1–10 s^{-1}, based on a kinetic study of DnaJ-catalyzed γ-phosphate cleavage by DnaK (McCarty et al., 1995).
- The rate constant k_{34} represents the release of inorganic phosphate from mHsp70. Because this process appears to be rapid (Dekker and Pfanner, 1997), we chose $k_{34} = 10$–100 s^{-1}.
- The rate constant k_{45} for the binding of mGrpE to mHsp70 was set equal to k_{23} at 1–10 s^{-1}, based on the observation that GrpE mediates exchange of DnaK-bound nucleotide on the same time scale that DnaJ catalyzes γ-phosphate cleavage by DnaK (McCarty et al., 1995).
- In the power stroke model, we multiplied k_{45} by the factor exp $[(p/20) - 5]$, where p is the percentage of the distance that would be covered if the power stroke went to completion. Although the form of this equation is arbitrary, the purpose was to make the power stroke mechanism efficient. We have modeled the mHsp70 power stroke as a

relaxing spring; therefore, the force of the power stroke decays exponentially as the stroke progresses, so most of the work of translocation is done in the first stages of the power stroke. By causing k_{45} to increase progressively during the power stroke, we allowed mHsp70 to remain bound to the chain when the motor was strongest and to dissociate from the chain as the motor became weaker.

- The rate constant k_{51} represents the ATP-driven displacement of mGrpE from mHsp70 and the subsequent dissociation of mHsp70 from the chain. Because this two-stage reaction will be slower than the simple dissociation of mHsp70 from the chain, k_{51} will be smaller than k_{21}, so we chose $k_{51} = 0.2–2\ s^{-1}$. These values are consistent with measurements from a recent study of the DnaK chaperone system (Pierpaoli et al., 1997).

APPENDIX D: MODEL EQUATIONS

The mathematical model consists of two parts: 1) a Markov chain representing the progress of the ATPase reaction cycle, and 2) the equations of motion for the chain in each state.

Denote the states of the Markov chain by $m = 1, 2, \ldots, 5$. The mean residence time in each state is given by the reciprocal of the rate constants for exiting from the state. Thus the kinetic chain is modeled by the state transition equations:

$$\frac{d\mathbf{s}}{dt} = \mathbf{M}\mathbf{s} \tag{D1}$$

where $\mathbf{s} = (s_1, s_2, \ldots, s_5)$ locates the system in kinetic states 1, 2, . . . , 5, and the transition matrix, M_{ij}, giving the probability of jumping from state i to state j is computed in the usual way: choose a random number, R, in the unit interval (0, 1); if $[1 - \exp(-k_{ij}\Delta t)] < R$, remain in the state for the next Δt, otherwise move to the next state. The transitions between states are considered to be instantaneous.

While in each state, we model the motion of the peptide chain as a Langevin equation, neglecting chain inertia:

$$\frac{dx_m}{dt} = \frac{D}{k_B T} F_m + B(t), \quad m = 1, 2, \ldots, 5, \tag{D2}$$

where $B(t)$ is the force due to Brownian fluctuations with the standard properties (Riskin, 1989): $\langle B(t)\rangle = 0$, $\langle B(t)B(t')\rangle = 2D\delta(t - t')$. The F_k are the forces acting on the chain, and D is the effective diffusion coefficient of the chain. The magnitude of D is computed from the data as described in Appendix B. This equation is simulated numerically by an Euler discretization:

$$x(t + \Delta t) = x(t) + \frac{D\Delta t}{k_B T} \sum F_k + \frac{\sqrt{2D\Delta t}N(0, 1)}{B(t)}, \tag{D3}$$

where $N(0, 1)$ is a Gaussian (normal) distribution with zero mean and unit variance, and Δt is the time step (Doering, 1990; Riskin, 1989).

In each state, the forces, F_k, acting on the chain are different. We can group the five kinetic states into three "dynamic" states (see Figs. 2–4). In the free state, $F_k = 0$, and the chain is free to diffuse. In the bound state, $D = 0$, and the chain is immobile. In the ratcheted state, backward movements of the chain are prohibited; we model this effect as a reflecting boundary condition at the chain end, $x = 0$, where mHsp70 has bound. In the power stroke state, the force is the spring force, $k(x - x_0)$, $x \geq 0$, where $k = 1.5$ pN/nm.

Thanks to Andreas Matouschek, Dean Astumian, Steve Kron, and Susan Lindquist for helpful feedback on the manuscript.

J-FC was partially supported by a Lavoisier Fellowship. GO was supported by NSF grant DMS 9220719. BSG was supported by grants from the Diabetes Research Foundation, the March of Dimes Birth Defects Foundation, the Cancer Research Foundation, and the Pew Scholars Program.

REFERENCES

Azem, A., W. Oppliger, A. Lustig, P. Jenö, B. Feifel, G. Schatz, and M. Horst. 1997. The mitochondrial hsp70 chaperone system: effect of adenine nucleotides, peptide substrate, and mGrpE on the oligomeric state of mhsp70. *J. Biol. Chem.* 272:20901–20906.

Blond-Elguindi, S., S. E. Cwirla, W. J. Dower, R. J. Lipshutz, S. R. Sprang, J. F. Sambrook, and M.-J. H. Gething. 1993. Affinity panning of a library of peptides displayed on bacteriophages reveals the binding specificity of BiP. *Cell.* 75:717–728.

Bolliger, L., O. Deloche, B. S. Glick, C. Georgopoulos, P. Jenö, N. Kronidou, M. Horst, N. Morishima, and G. Schatz. 1994. A mitochondrial homolog of bacterial GrpE interacts with mitochondrial hsp70 and is essential for viability. *EMBO J.* 13:1998–2006.

Bömer, U., M. Meijer, A. C. Maarse, A. Hönlinger, P. J. T. Dekker, N. Pfanner, and J. Rassow. 1997. Multiple interactions of components mediating preprotein translocation across the inner mitochondrial membrane. *EMBO J.* 16:2205–2216.

Boorstein, W. R., T. Ziegelhoffer, and E. A. Craig. 1994. Molecular evolution of the HSP70 multigene family. *J. Mol. Evol.* 38:1–17.

Coppin, C. M., J. T. Finer, J. A. Spudich, and R. D. Vale. 1995. Measurement of the isometric force exerted by a single kinesin molecule. *Biophys. J.* 68:242S–244S.

Creighton, T. 1993. *Proteins.* W. H. Freeman, New York.

Dekker, P. J. T., and N. Pfanner. 1997. Role of mitochondrial GrpE and phosphate in the ATPase cycle of matrix Hsp70. *J. Mol. Biol.* 270: 321–327.

Doering, C. 1990. Modeling complex systems: stochastic processes, stochastic differential equations, and Fokker-Planck equations. *In* 1990 Lectures in Complex Systems. L. Nadel and D. Stein, editors. Addison-Wesley, Redwood City, CA. 3–51.

Doi, M., and S. Edwards. 1986. The Theory of Polymer Dynamics. Oxford University Press, New York.

Eilers, M., S. Hwang, and G. Schatz. 1988. Unfolding and refolding of a purified precursor protein during import into mitochondria. *EMBO J.* 7:1139–1145.

Finer, J. T., A. D. Mehta, and J. A. Spudich. 1995. Characterization of single actin-myosin interactions. *Biophys. J.* 68:291S–297S.

Finer, J. T., R. M. Simmons, and J. A. Spudich. 1994. Single myosin molecule mechanics: piconewton forces and nanometre steps. *Nature.* 368:113–119.

Flynn, G. C., J. Pohl, M. T. Flocco, and J. E. Rothman. 1991. Peptide-binding specificity of the molecular chaperone BiP. *Nature.* 353: 726–730.

Gambill, B. D., W. Voos, P. J. Kang, B. Miao, T. Langer, E. A. Craig, and N. Pfanner. 1993. A dual role for mitochondrial heat shock protein 70 in membrane translocation of preproteins. *J. Cell Biol.* 123:109–117.

Glick, B. S. 1995. Can Hsp70 proteins act as force-generating motors? *Cell.* 80:11–14.

Glick, B. S., A. Brandt, K. Cunningham, S. Müller, R. L. Hallberg, and G. Schatz. 1992. Cytochromes c_1 and b_2 are sorted to the intermembrane space of yeast mitochondria by a stop-transfer mechanism. *Cell.* 69: 809–822.

Glick, B. S., C. Wachter, G. A. Reid, and G. Schatz. 1993. Import of cytochrome b_2 to the mitochondrial intermembrane space: the tightly folded heme-binding domain makes import dependent upon matrix ATP. *Protein Sci.* 2:1901–1917.

Gragerov, A., and M. E. Gottesman. 1994. Different peptide binding specificities of hsp70 family members. *J. Mol. Biol.* 241:133–135.

Greene, L. E., R. Zinner, S. Naficy, and E. Eisenberg. 1995. Effect of nucleotide on the binding of peptides to 70-kDa heat shock protein. *J. Biol. Chem.* 270:2967–2973.

Harrison, C. J., M. Hayer-Hartl, M. Di Liberto, F.-U. Hartl, and J. Kuriyan. 1997. Crystal structure of the nucleotide exchange factor GrpE bound to the ATPase domain of the molecular chaperone DnaK. *Science.* 276: 431–435.

Horst, M., A. Azem, G. Schatz, and B. S. Glick. 1997. What is the driving force for protein import into mitochondria? *Biochim. Biophys. Acta.* 1318:71–78.

Horst, M., W. Oppliger, B. Feifel, G. Schatz, and B. S. Glick. 1996. The mitochondrial protein import motor: dissociation of mitochondrial hsp70 from its membrane anchor requires ATP binding rather than ATP hydrolysis. *Protein Sci.* 5:759–767.

Hunt, A., F. Gittes, and J. Howard. 1994. The force exerted by single kinesin molecule against a viscous load. *Biophys. J.* 67:766–781.

Hurt, E. C., B. Pesold-Hurt, and G. Schatz. 1984. The cleavable prepiece of an imported mitochondrial protein is sufficient to direct cytosolic dihydrofolate reductase into the mitochondrial matrix. *FEBS Lett.* 178: 306–310.

Huxley, A., and R. Simmons. 1971. Proposed mechanism of force generation in striated muscle. *Nature.* 233:533–538.

Hwang, S. T., and G. Schatz. 1989. Translocation of proteins across the mitochondrial inner membrane, but not into the outer membrane, requires nucleoside triphosphates in the matrix. *Proc. Natl. Acad. Sci. USA.* 86:8432–8436.

Hwang, S. T., C. Wachter, and G. Schatz. 1991. Protein import into the yeast mitochondrial matrix. A new translocation intermediate between the two mitochondrial membranes. *J. Biol. Chem.* 266:21083–21089.

Jordan, R., and R. McMacken. 1995. Modulation of the ATPase activity of the molecular chaperone DnaK by peptides and the DnaJ and GrpE heat shock proteins. *J. Biol. Chem.* 270:4563–4569.

Kang, P.-J., J. Ostermann, J. Shilling, W. Neupert, E. A. Craig, and N. Pfanner. 1990. Requirement for hsp70 in the mitochondrial matrix for translocation and folding of precursor proteins. *Nature.* 348:137–143.

Karzai, A. W., and R. McMacken. 1996. A bipartite signaling mechanism involved in DnaJ-mediated activation of *Escherichia coli* DnaK protein. *J. Biol. Chem.* 271:11236–11246.

Kronidou, N. G., W. Oppliger, L. Bolliger, K. Hannavy, B. S. Glick, G. Schatz, and M. Horst. 1994. Dynamic interaction between Isp45 and mitochondrial hsp70 in the protein import system of the yeast mitochondrial inner membrane. *Proc. Natl. Acad. Sci. USA.* 91:12818–12822.

Laloraya, S., P. J. T. Dekker, W. Voos, E. A. Craig, and N. Pfanner. 1995. Mitochondrial GrpE modulates the function of matrix Hsp70 in translocation and maturation of preproteins. *Mol. Cell. Biol.* 15:7098–7105.

Laloraya, S., B. D. Gambill, and E. A. Craig. 1994. A role for a eukaryotic GrpE-related protein, Mge1p, in protein translocation. *Proc. Natl. Acad. Sci. USA.* 91:6481–6485.

Liberek, K., J. Marszalek, D. Ang, C. Georgopoulos, and M. Zylicz. 1991. *Escherichia coli* DnaJ and GrpE heat shock proteins jointly stimulate ATPase activity of DnaJ. *Proc. Natl. Acad. Sci. USA.* 88:2874–2878.

Lill, R., F. E. Nargang, and W. Neupert. 1996. Biogenesis of mitochondrial proteins. *Curr. Opin. Cell Biol.* 8:505–512.

Matouschek, A., A. Azem, K. Ratliff, B. S. Glick, K. Schmid, and G. Schatz. 1997. Active unfolding of precursor proteins during mitochondrial protein import. *EMBO J.* 16:6727–6736.

Matouschek, A., S. Rospert, K. Schmid, B. S. Glick, and G. Schatz. 1995. Cyclophilin catalyzes protein folding in yeast mitochondria. *Proc. Natl. Acad. Sci. USA.* 92:6319–6323.

Mayer, A., W. Neupert, and R. Lill. 1995. Mitochondrial protein import: reversible binding of the presequence at the *trans* side of the outer membrane drives partial translocation and unfolding. *Cell.* 80:127–137.

McCarty, J. S., A. Buchberger, J. Reinstein, and B. Bukau. 1995. The role of ATP in the functional cycle of the DnaK chaperone system. *J. Mol. Biol.* 249:126–137.

Miao, B., J. E. Davis, and E. A. Craig. 1997. Mge1 functions as a nucleotide release factor for Ssc1, a mitochondrial Hsp70 of *Saccharomyces cerevisiae. J. Mol. Biol.* 265:541–552.

Nakai, M., Y. Kato, E. Ikeda, A. Toh-e, and T. Endo. 1994. Yge1p, a eukaryotic GrpE homolog, is localized in the mitochondrial matrix and interacts with mitochondrial Hsp70. *Biochem. Biophys. Res. Commun.* 200:435–442.

Neupert, W., F.-U. Hartl, E. A. Craig, and N. Pfanner. 1990. How do polypeptides cross the mitochondrial membranes? *Cell.* 63:447–450.

Park, P., and W. Sung. 1996. Polymer translocation through a membrane pore. *Phys. Rev. Lett.* 77:783–786.

Peskin, C., G. Odell, and G. Oster. 1993. Cellular motions and thermal fluctuations: the Brownian ratchet. *Biophys. J.* 65:316–324.

Peskin, C., and G. Oster. 1995. Coordinated hydrolysis explains the mechanical behavior of kinesin. *Biophys. J.* 68:202S–210S.

Pfanner, N., and M. Meijer. 1995. Pulling in the proteins. *Curr. Biol.* 5:132–135.

Pierpaoli, E. V., E. Sandmeier, A. Baici, H.-J. Schönfeld, S. Gisler, and P. Christen. 1997. The power stroke of the DnaK/DnaJ/GrpE molecular chaperone system. *J. Mol. Biol.* 269:757–768.

Rassow, J., F.-U. Hartl, B. Guiard, N. Pfanner, and W. Neupert. 1990. Polypeptides traverse the mitochondrial envelope in an extended state. *FEBS Lett.* 275:190–194.

Rassow, J., A. C. Maarse, E. Krainer, M. Kübrich, H. Müller, M. Meijer, E. A. Craig, and N. Pfanner. 1994. Mitochondrial protein import: biochemical and genetic evidence for interaction of matrix hsp70 and the inner membrane protein MIM44. *J. Cell Biol.* 127:1547–1556.

Rensing, S. A., and U. G. Maier. 1994. Phylogenetic analysis of the stress-70 protein family. *J. Mol. Evol.* 39:80–86.

Riskin, H. 1989. The Fokker-Planck Equation. Springer-Verlag, New York.

Rowley, N., C. Prip-Buus, B. Westermann, C. Brown, E. Schwarz, B. Barrell, and W. Neupert. 1994. Mdj1p, a novel chaperone of the DnaJ family, is involved in mitochondrial biogenesis and protein folding. *Cell.* 77:249–259.

Schatz, G., and B. Dobberstein. 1996. Common principles of protein translocation across membranes. *Science.* 271:1519–1526.

Scherer, P. E., U. C. Krieg, S. T. Hwang, D. Vestweber, and G. Schatz. 1990. A precursor protein partly translocated into yeast mitochondria is bound to a 70 kd mitochondrial stress protein. *EMBO J.* 9:4315–4322.

Schleyer, M., and W. Neupert. 1985. Transport of proteins into mitochondria: translocational intermediates spanning contact sites between outer and inner membranes. *Cell.* 43:339–350.

Schmid, D., A. Baici, H. Gehring, and P. Christen. 1994. Kinetics of molecular chaperone action. *Science.* 263:971–973.

Schneider, H., J. Berthold, M. F. Bauer, K. Dietmeier, B. Guiard, M. Brunner, and W. Neupert. 1994. Mitochondrial Hsp70/MIM44 complex facilitates protein import. *Nature.* 371:768–774.

Schneider, H.-C., B. Westermann, W. Neupert, and M. Brunner. 1996. The nucleotide exchange factor MGE exerts a key function in the ATP-dependent cycle of mt-Hsp70-Tim44 interaction driving mitochondrial protein import. *EMBO J.* 15:5796–5803.

Schnitzer, M., and S. Block. 1995. Statistical kinetics of processive enzymes. *Cold Spring Harb. Symp. Quant. Biol.* 60:793–802.

Simon, S. M., C. S. Peskin, and G. F. Oster. 1992. What drives the translocation of proteins? *Proc. Natl. Acad. Sci. USA.* 89:3770–3774.

Spudich, J. A. 1994. How molecular motors work. *Nature.* 372:515–518.

Stuart, R. A., D. M. Cyr, E. A. Craig, and W. Neupert. 1994. Mitochondrial molecular chaperones: their role in protein translocation. *Trends Biochem. Sci.* 19:87–92.

Svodoba, K., and S. Block. 1994. Force and velocity measured for single kinesin molecules. *Cell.* 77:773–784.

Svodoba, K., P. Mitra, and S. Block. 1994. Fluctuation analysis of motor protein movement and single enzyme kinetics. *Proc. Natl. Acad. Sci. USA.* 91:11782–11786.

Szabo, A., T. Langer, H. Schröder, J. Flanagan, B. Bukau, and F. U. Hartl. 1994. The ATP hydrolysis-dependent reaction cycle of the *Escherichia coli* Hsp70 system—DnaK, DnaJ, and GrpE. *Proc. Natl. Acad. Sci. USA.* 91:10345–10349.

Ungermann, C., B. Guiard, W. Neupert, and D. M. Cyr. 1996. The $\Delta\Psi$ and Hsp70/MIM44-dependent reaction cycle driving early steps of protein import into mitochondria. *EMBO J.* 15:734–744.

Ungermann, C., W. Neupert, and D. M. Cyr. 1994. The role of Hsp70 in conferring unidirectionality on protein translocation into mitochondria. *Science.* 266:1250–1253.

Vale, R. D. 1994. Getting a grip on myosin. *Cell.* 78:733–737.

Vestweber, D., and G. Schatz. 1988a. A chimeric mitochondrial precursor protein with internal disulfide bridges blocks import of authentic precursors into mitochondria and allows quantitation of import sites. *J. Cell Biol.* 107:2037–2043.

Vestweber, D., and G. Schatz. 1988b. Mitochondria can import artificial precursor proteins containing a branched polypeptide chain or a carboxy-terminal stilbene disulfonate. *J. Cell Biol.* 107:2045–2049.

Vestweber, D., and G. Schatz. 1989. DNA-protein conjugates can enter mitochondria via the protein import pathway. *Nature.* 338:170–172.

von Ahnsen, O., W. Voos, H. Henninger, and N. Pfanner. 1995. The mitochondrial protein import machinery. Role of ATP in dissociation of the Hsp70-Mim44 complex. *J. Biol. Chem.* 270:29848–29853.

Voos, W., B. D. Gambill, B. Guiard, N. Pfanner, and E. A. Craig. 1993. Presequence and mature part of preproteins strongly influence the dependence of mitochondrial protein import on heat shock protein 70 in the matrix. *J. Cell Biol.* 123:119–126.

Wachter, C., G. Schatz, and B. S. Glick. 1992. Role of ATP in the intramitochondrial sorting of cytochrome c_1 and the adenine nucleotide translocator. *EMBO J.* 11:4787–4794.

Wachter, C., G. Schatz, and B. S. Glick. 1994. Protein import into mitochondria: the requirement for external ATP is precursor-specific whereas intramitochondrial ATP is universally needed for translocation into the matrix. *Mol. Biol. Cell.* 5:465–474.

Wang, H.-Y., T. Elston, A. Mogilner, and G. Oster. 1997. Force generation in RNA polymerase. *Biophys. J.* (in press).

Wienhues, W., K. Becker, M. Schleyer, B. Guiard, M. Tropschug, A. L. Horwich, N. Pfanner, and W. Neupert. 1991. Protein folding causes an arrest of preprotein translocation into mitochondria in vivo. *J. Cell Biol.* 115:1601–1609.

Zhu, X., X. Zhao, W. F. Burkholder, A. Gragerov, C. M. Ogata, M. E. Gottesman, and W. A. Hendrickson. 1996. Structural analysis of substrate binding by the molecular chaperone DnaK. *Science.* 272: 1606–1614.